Comprehensive chemical description of pyrolysis chars from low-density polyethylene (LDPE) by thermal analysis hyphenated to different mass spectrometric approaches

Lukas Friederici[1,2], Eric Schneider[1,2], Gaëtan Burnens[3,4], Thorsten Streibel[1,5], Pierre Giusti[4,6], Christopher P. Rüger*[1,2,4], Ralf Zimmermann[1,2,5]

1 –Joint Mass Spectrometry Centre (JMSC)/Chair of Analytical Chemistry, University of Rostock, 18059 Rostock, Germany

2 – Department Life, Light & Matter (LLM), University of Rostock, 18051 Rostock, Germany

3 – TotalEnergies, Total Research and Technology Feluy (TRTF), B-7181 Feluy, Belgium

4 – International Joint Laboratory−iC2MC: Complex Matrices Molecular Characterization, TotalEnergies - TRTG Refining and Chemicals, Gonfreville l'Orcher, 76700 Harfleur, France

5 – Joint Mass Spectrometry Centre (JMSC)/Helmholtz Zentrum München, Comprehensive Molecular Analytics, 85764 Neuherberg, Germany

6 – TotalEnergies, TRTG Refining and Chemicals, Gonfreville l'Orcher, 76700 Harfleur, France

* – corresponding author, christopher.rueger@uni-rostock.de

Keywords

pyrolysis, recycling, coke, thermal analysis, mass spectrometry, polyethylene

Table of content only

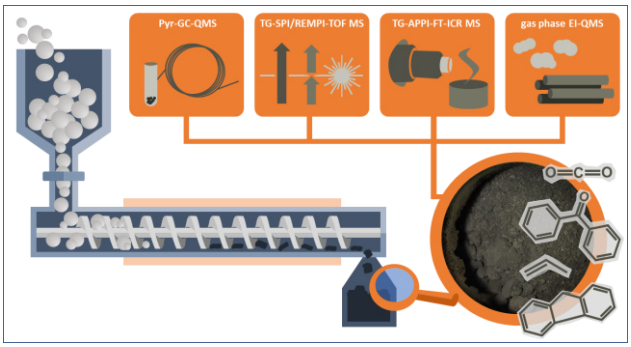

Abstract

In the last decades the production and demand of plastics has drastically increased, with severe environmental impact. Concerning climate change and the idea of a circular economy, waste incineration is not favored, and efficient recycling strategies are needed. As one of the most promising approaches, pyrolysis generates a certain amount of solid residue besides liquid and gaseous products. The chemical nature of this coke is not fully understood, but it holds the potential to be used in material science or to generate further chemicals. To explore the value of this feedstock, thermal analysis with mass spectrometric detection of the evolved gas mixture is deployed. With the help of soft photoionization techniques, we were able to identify alkenes, dienes, and polycyclic aromatic hydrocarbons (PAHs), which were emitted at four distinct mass loss events. Here, resonance-enhanced multiphoton ionization allows selectively addressing the aromatic constituents, whereas single-photon ionization covered a comprehensive chemical range. Interestingly, we found an enrichment of UV-stabilizers, such as benzophenone, within the macromolecular nature of the residue. The evolved gas mixture was found to be highly complex. Consequently, high-resolution mass spectrometry addressing the isobaric complexity and pyrolysis gas chromatography was used for structural elucidation. We hypothesize island- and archipelago-type structural motives comparable to asphaltenes but with almost no heteroatoms based on analyzing the complex mixture by carbon number versus double bond equivalent cartographies. A comprehensive set of thermal analysis mass spectrometric platforms enabled an in-depth chemical description of plastic pyrolysis coke, valuable knowledge in reactor design and material science.

Introduction

The handling of waste, and in particular of plastic waste, confronts humankind with one of the greatest challenges of the current century. Efficient recycling and reuse strategies will be a key for reducing carbon dioxide emissions and tackling climate change as well as ecological problems. Plastic is one of the most important materials and ubiquitous in our daily lives; its global production has increased twentyfold since the 1960s. [1] Accompanied by this demand, over 29.1 million tons of plastic waste are generated in Europe every year with a high rate of landfilling and incineration. [1] Consequently, the key aspects are regulating the production and consumption of plastics; reusing plastic products or replacing plastic with other materials. Nonetheless, modern society and the economy will still face a substantial usage of plastics. In 2018, the European Commission announced to focus towards fully recyclable plastic packaging by 2030 [1,2], and at the beginning of 2021, the European Union even introduced a plastics tax of 800 €/t [3] on plastic packaging that is not recycled.

Aside from mechanical recycling, chopping, grinding, and melting the waste, one of the most promising strategies for treating waste plastics is pyrolysis. [4] Certain polymers can also be chemically recycled, such as polyethylene terephthalate, but this demands relatively pure educts, which is uncommon for solid plastic waste (SPW). Plenty of research was conducted in understanding the thermal and catalytic pyrolysis of waste plastics into valuable chemicals. [5] Most often, fuel-like hydrocarbons or the respective monomeric building blocks are targeted. Historically, the lower price of secondary raw materials compared to primary raw materials were making plastic pyrolysis economically unappealing and hindered huge investment by the industry. In the last two decades, new legislation, along with voluntary actions by major producers and users of plastics, changed this picture and the demand for recycled plastics is drastically increasing.

Generally, pyrolysis of SPW will result in hydrocarbon-rich gas, a liquid oil, and coke (solid residues). [6] The pyrolysis conditions and raw material largely affect the product composition. Most often, higher pyrolysis temperatures will result in a higher yield of gaseous components. [6] Nonetheless, reactor design, residence time, and temperature protocol also cause a substantial impact. [7] Hence, understanding the mechanisms allows for designing optimized recycling strategies and making a circular economy possible. Thermal analysis techniques, such as thermogravimetric analysis (TGA), are frequently conducted prior to real pyrolysis experiments at a pyrolysis plant or reactor. [8] Those TGA experiments allow simulating the pyrolysis at a laboratory scale. Information on the general thermal behavior of the feed material can be gained to tune the real reaction conditions. [9,10]

In a previous study, we could show that the pyrolysis degradation mechanism of rather simple polymers, such as pure PET, can be highly diverse and yield extremely complex mixtures. [11] This

problem creates the demand for suitable analytical techniques to unravel the chemical composition on a molecular level. For the detection of gaseous components established online techniques exist allowing for good qualitative and quantitative insight. [12,13] A characteristic target is the yield of benzene, toluene, and xylene (BTX aromatics). The situation is getting more complex when analyzing the liquid plastic pyrolysis products. Here a limited number of routine protocols exist yielding the desired molecular information. In literature, soft atmospheric pressure ionization, such as electrospray ionization (ESI), with high-resolution mass spectrometric detection [14] is discussed but also other spectroscopic [15] and chromatographic [16] attempts exist.

Not much attention has been paid to the pyrolysis coke itself. When it comes to the solid residues of pyrolytic plastic recycling, very limited studies on a comprehensive chemical description are published. Commonly, bulk-properties and physical parameters are determined, such as bulk elemental composition [16], morphology/microscopy, rheological properties, and surface area (porosity). [17,18] The solid residue was mentioned to be used as a raw material to produce activated carbon but also as a feed for further gasification or the generation of other liquid chemicals. [17] Spectroscopic attempts, such as Fourier transform infrared spectroscopy (FT-IR) or nuclear magnetic resonance (NMR) spectroscopy, have been made to describe the solid material on a molecular level. [19–21] With these approaches, the dominant chemical functionalities can be well described. Despite the existence of mass spectrometric approaches, *e.g.*, by laser desorption ionization of solid materials, such as coal or bitumen, there is a research gap in the molecular understanding of the solid residue and the chemicals bound by the highly aromatic graphitized matrix.

This research aimed to study the chemical composition of solid residue (coke) of plastic pyrolysis deploying state-of-the-art mass spectrometric concepts. As a first attempt, we focus on a simple but crucial case, the pyrolytic treatment of low-density polyethylene (LDPE). LDPE is produced in multi-millions tons annually [4], primarily used in packaging and consumer products, and accounts for over 20 w-% of the total plastic present in municipal solid waste, but has very low recycling rates commonly below 10 w-%. Evolved gas analysis approaches coupled with powerful mass spectrometric instrumentation have shown great potential to study solid and high-viscous complex organic mixtures, such as bitumen, polymers and asphaltenes. Hence, we deployed a set of different thermal analysis methods coupled to mass spectrometric detection with specialized ionization approaches allowing access to different parts of the compositional and chemical space. Pyrolysis gas chromatography acts as established technique yielding isomeric information. In contrast, more specific techniques, such as resonance-enhanced multiphoton or single-photon ionization (REMPI/SPI), are able to selectively and sensitively address aromatic constituents or act as an almost universal ionization approach, respectively. [22,23] Ultimately, high-resolution mass spectrometry allowed to address the isobaric complexity of the evolved pattern. This work aimed to address two main research questions: 1) Can

we describe the chemical fingerprint of the evaporable fraction of the pyrolysis coke, and 2) can the raw residue coke be further thermally treated to generate valuable products in respect of a circular economy? Aside from these economical aspects, the information on the chemical composition of the coke is crucial for judging the ecological risks of the coke to human health and the environment. In this connection, primarily polycyclic aromatic hydrocarbons (PAHs) with their high carcinogenicity and mutagenicity are of particular interest [24].

Experimental Section

Material

In this study, five coke samples generated from a prototype pyrolysis reactor were investigated. The pilot plant was fed with unmixed solid plastic waste (SPW) composed of low-density polyethylene (LDPE) continuously pyrolyzed at 410 °C. Different reactor operation parameters were adapted and changed. In this respect, the type of atmosphere (nitrogen, argon), the reactor mass loading, and the rotational speed of the tubular reactor were changed. The samples were provided by Total Petrochemicals Feluy SA (TRTF – Total Research & Technology Feluy, Belgium). Details on the coke materials and reactor settings are given in Table S1.

Instrumentation

Four thermal analysis setups coupled to different mass spectrometric platforms were deployed within this study: (1/4) thermogravimetry vacuum photoionization with time-of-flight mass spectrometric detection (TG REMPI/SPI ToF MS), (2/4) thermogravimetry atmospheric pressure photoionization ultrahigh-resolution mass spectrometry (TG APPI FT-ICR MS), (3/4) thermogravimetry with electron ionization and quadrupole mass spectrometric detection (TG EI QMS) [25–27] and (4/4) pyrolysis gas chromatography with electron ionization and quadrupole mass spectrometric detection (Pyr GC EI QMS). Technical details and schemes of the different mass spectrometric platforms are given elsewhere. [28]

For the first setup (1/4), a simultaneous thermal analyzer (STA7200RV, Hitachi) was coupled to a custom photoionization time-of-flight mass spectrometer, which utilizes SPI and REMPI. A few milligrams (1−3 mg) of the sample material were placed in a corundum crucible (Al_2O_3). Thermal analysis was carried out with a heating rate of 20 K/min under an inert nitrogen atmosphere (200 mL/min) from 40 to 900 °C. Evolving constituents of the effluent from the thermal analyzer were sampled via a heated interface and transfer line (3.50 m length and 200 µm inner diameter at 250 °C). In brief, for SPI, 355 nm laser pulses (25 mJ pulse energy, 10 Hz repetition rate, and 5 ns pulse width), generated from a Nd:YAG laser (Surelite III, Continuum, Inc., SantaClara, CA, U.S.A.), were sent through a xenon-filled gas cell (Xe 4.0, 12 mbar), yielding vacuum ultraviolet photons by nonlinear frequency

tripling (118 nm, 10.5 eV). For REMPI, 266 nm laser pulses were employed, generated from the same laser through frequency quadrupling. The molecular ions formed after soft photoionization are recorded with an acquisition frequency of 10 Hz from *m/z* 5−500 with a reflectron TOF-MS (Stefan Kaesdorf, Munich, Germany) using a multichannel plate detector. [29,30]

The second mass spectrometric hyphenation (2/4) is composed of a thermobalance (TG 209, Netzsch Gerätebau, Selb, Germany) coupled to a modified Bruker GC-APCI II source equipped with atmospheric pressure photoionization (APPI) by a Kr vacuum ultraviolet lamp (10/10.6 eV, 124/117 nm) as a soft ionization technique preserving the molecular pattern. [31] The temperature program of the thermobalance with a constant flow of 200 mL/min nitrogen was 2 min isothermal at 20 °C, ramp to 600 °C with 10 K/min, and hold for 10 min at 600 °C. The evolved mixture was sampled via a 300 °C interface and 280 °C transfer line (deactivated fused silica capillary, 0.53 mm ID, 300 °C) into the ion source of the mass spectrometer. For mass spectrometric detection, a Bruker Apex II ultra FT−MS equipped with a 7 T superconducting magnet was used. Mass spectra were recorded from *m/z* 100 to 1000 with a four mega word transient, resulting in resolving power of roughly 300 000 at *m/z* 400. Time-resolved broadband spectra each with ten micro scans were recorded. A detailed description of the setup can be found elsewhere. [28,30]

The third setup (3/4) is a hyphenation of a quadrupole mass spectrometer with electron ionization to the thermobalance used in the second setup. For the TG EI QMS analysis corundum crucibles (Al_2O_3) were used. Evolving constituents of the effluent from the thermal analyzer were sampled via an unheated interface and transfer line (3 m length and 10 µm inner diameter) and ionized by 70 eV. The following selected ion traces were detected: *m/z* 15, 17, 18, 26, 30, 34, 42, 44. [25]

For the last setup (4/4), pyrolysis gas chromatographic analysis was applied. Roughly 0.5−0.9 mg of the solid sample was injected into the pyrolyzer (model PY-2020iD, double-shot pyrolyzer, Frontier Laboratories) mounted onto an HP 6890 gas chromatograph. The sample material undergoes a pyrolysis step at 600 °C, held for 1 min. To separate the evolved gas mixture, a 30 m SGE-BPX5 column (250 µm inner diameter, 0.25 µm film, helium at 99.999%, and head pressure at 0.4 bar, split of 1:50) was used. The following temperature program was applied: hold for 10 min at 40 °C, ramp to 330 °C with 10 K/min, and hold for 5 min. The effluent from the column was ionized by 70 eV electron ionization and analyzed by a quadrupole mass spectrometer. Mass spectra were recorded in scan mode from *m/z* 40–500. [28,32,33]

Mass spectrometric data analysis

For 1/4 data processing and analysis were carried out with the instrument-specific LabView (2014) graphical user interface. For 2/4: External calibration of the mass spectra was performed using a

polystyrene standard. Afterward, an internal calibration utilizing characteristic CHO homolog rows were performed, each scan of the time-resolved data was peak picked (S/N 6) and exported with a visual basic script in Bruker Data Analysis 5.0 (Bruker Daltoniks, Bremen, Germany). The exported mass spectra were processed by self-written MATLAB algorithms and routines combined in a graphical user interface named CERES Processing. After careful manual investigation, the following restrictions were deployed for elemental composition assignment: CcHhNnOoSs; $6 \leq c \leq 70$, $6 \leq h \leq 100$, $n \leq 1$, $o \leq 8$, and $s \leq 0$ with a maximal error of 1 ppm. For the analysis and visualization (TG EI QMS/Pyr GC EI QMS) self-written MATLAB R2019b functions were used in combination with a MATLAB-based graphical user interface (CERES Viewer).

Results and Discussion

First physicochemical information about the five pyrolysis coke samples is gained by the thermogravimetric data summarized in **Figure 1**. The thermogram correlates the time-resolved mass loss data from desorption or pyrolysis processes to a specific temperature. Generally, the coke samples reveal substantial mass loss between 100 and 800 °C. After the thermal treatment, a residue of 45 to 58 w-% remained, corresponding to pyrolytic carbon and inorganic constituents. Consequently, a second thermal treatment of the initial pyrolysis coke residue can substantially reduce the total amount of waste in the recycling process. The numeric derivation of the mass loss curve leads to the differential thermogravimetric (DTG) curve. It shows four distinct local maxima at 400 °C, 500 °C, 600 °C, and 750 °C. The feedstock material – unmixed solid LDPE waste – for the pyrolysis reactor is the same for all samples and consequently, a general similarity can be found between all coke residues. Despite variation in pyrolysis reactor parameters, the location of the maxima is for all samples approximately the same but differently pronounced.

The inhomogeneity of the sample material, due to their origin as by-products from the LDPE waste mixture pyrolysis, results in considerable variance of the measurements. This aspect also needs to be considered in a real-world scenario for the pyrolysis char utilization and potential upgrading. Here, to compensate this effect, a statistical outlier test (Grubb's test) [34] was applied to the thermal analysis data, and only the remaining measurements were used for the calculation of the mean value formation. The first peak at 390 °C shows the highest mass loss rate for Coke A and the lowest for Coke C, which correlates with the observed residual mass. The differences in the pyrolytic conditions are relatively low; primarily the reactor exit temperature is slightly reduced by about 10 °C for Coke A. In addition, the purge gas flow of the reactor was changed between Argon and Nitrogen. Argon may have a small influence on the production of pyrolysis char, leading to a reduced amount of residual mass (char), but this effect can be hypothesized to be minimal. Coke A shows the highest rate of mass loss for the second peak, closely followed by Coke B. For the remaining peaks, the difference between

the samples is much lower. Only Coke E and Coke B revealed a significant shift to slightly higher temperatures and a higher rate of mass loss at 500 °C. Consequently, the differences in the residual mass are mainly a result of the desorption and pyrolytic processes at temperatures below 550 °C. All five coke samples qualitatively show the same DTG profile. Consequently, the following discussion will focus on Coke A in detail.

The thermal analysis data suggest that the samples contain a significant but variable amount of defined structures that are decomposing during the heating, leading to rather sharp and defined mass loss steps. In contrast to these findings, earlier laboratory studies conducted with pure LDPE revealed only one mass loss step, which corresponds to the pyrolytic formation of smaller alkenes. [29] The pyrolysis coke shows unique thermal behavior, and chemical information on the evolved gas mixture is needed for an understanding of the processes and potential for utilization. Therefore, we applied two soft ionization schemes, SPI and REMPI, to the thermal balance for evolved gas analysis.

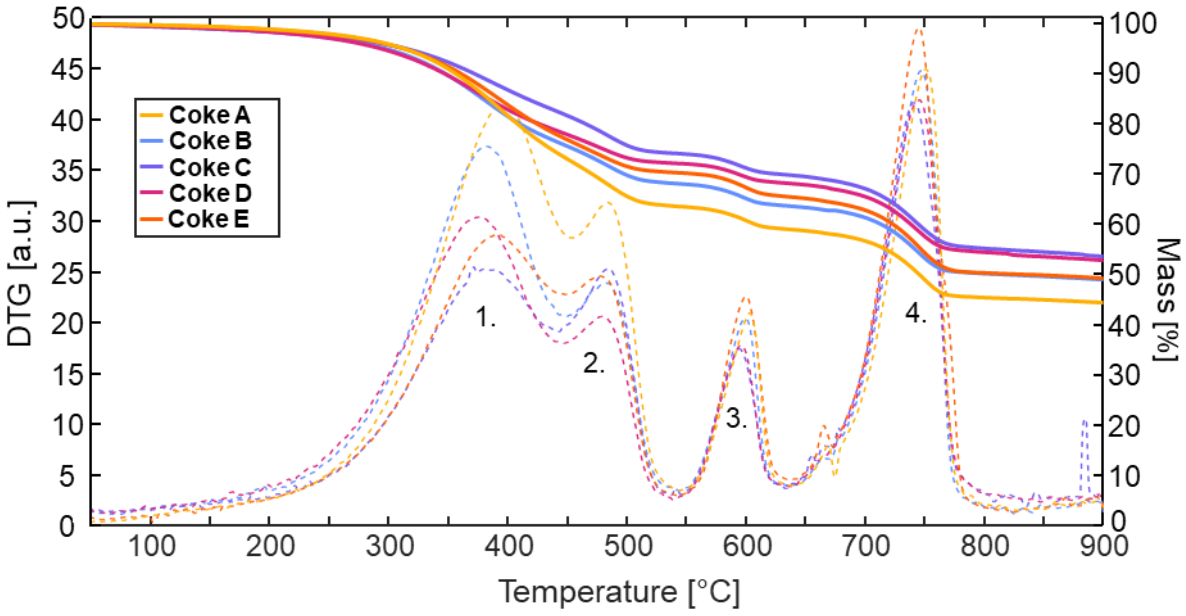

Figure 1. Mass loss (solid line) and differential thermogravimetric (DTG, dashed line) results of the plastic waste pyrolysis coke thermal investigation. Several distinct decomposition steps similar to all five coke samples but differently pronounced can be observed. Due to the similar nature of all pyrolysis coke samples, Coke A was selected for all further visualization.

These ionization techniques allow for an efficient description of the released molecules. With SPI at 118 nm, all molecules with an ionization potential below 10.5 eV can be ionized [35]. For the pyrolysis of LDPE, various alkenes are expected from the literature [6], and SPI allows to investigate a broad chemical space, including alkanes, alkenes and aromatics with different functionalities and structures.

[36,37] Moreover, also toxic aromatic constituents are formed during LDPE pyrolysis sensitively addressed by REMPI. Addressing a broad chemical space will also address the potential effects of plasticizers.

For both ionization schemes, three different major peaks at 300 °C, 500 °C and 600 °C are found in the total ion count signal (**Figure 2**). A huge discrepancy can be found by comparing the DTG curve with the total ion count signal (TIC) of both mass spectrometric techniques. No coincidence between the first peak of the SPI and REMPI signal and the DTG curve at approximately 400 °C is measured. Two overlapping release steps could cause this finding. With one containing volatile compounds that are desorbed from the sample at temperatures below pyrolysis (100-400 °C) and can be detected by SPI and REMPI. The second step, responsible for the majority of mass loss (below 400 °C), presumably produces smaller, volatile compounds that cannot or poorly (with low ionization cross-sections) be detected with the photoionization schemes; therefore not/hardly seen in the TICs. In the third event, the mass loss in the thermal balance is in the same temperature range as the mass spectrometric response. Between 700 and 800 °C, no distinct peak is observed in the mass spectrometric detection during the fourth mass loss step. Since the ionization energy decreases with the size/chain length of the molecules [38], the released molecules are more likely very small gaseous molecules.

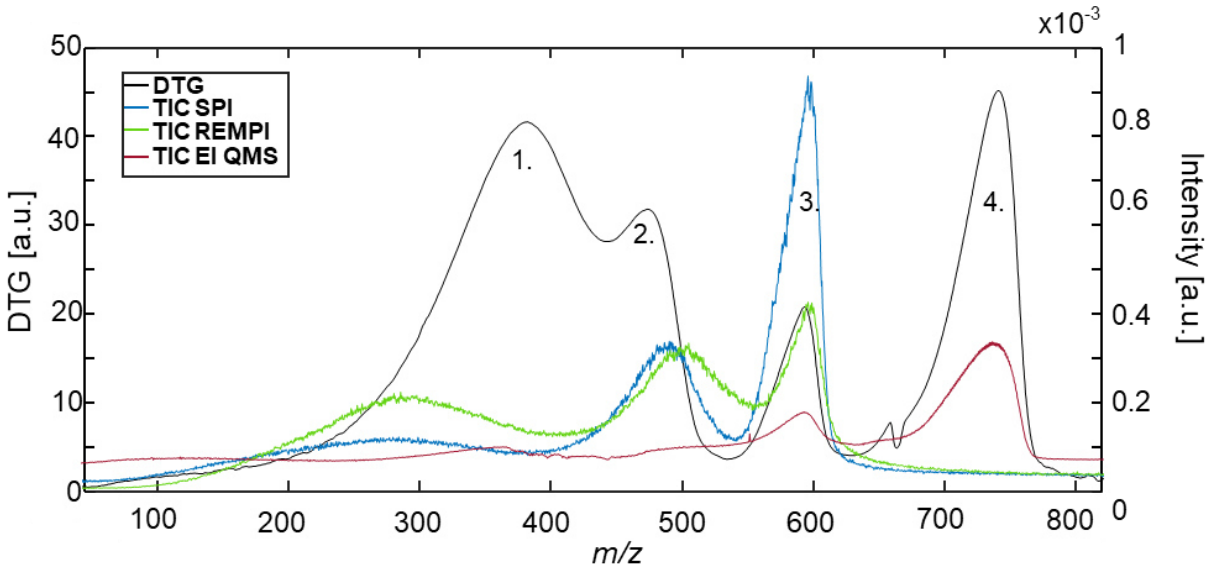

Figure 2. Overview of the TG-SPI/REMPI time-of-flight mass spectrometry results of Coke A and the analysis of light gases and small molecules by hyphenation of TG and QMS (The corresponding mass spectra are shown in **Figure S3**). Comparison of DTG and TIC curves with the three different mass spectrometric techniques (TG-SPI/REMPI and TG-EI-QMS).

This hypothesis was tested by direct coupling of the thermobalance with universal electron ionization and quadrupole mass spectrometric detection. A non-heated transferline was used avoiding sampling of the high-boiling point and very complex molecular pattern during the pyrolysis phase as seen in the photoionization mass spectra. This room-temperature sampling enabled a focus on light gases. The response of the mass spectrometer is in good agreement with the DTG data. Especially the fourth peak can be assigned to purely resulting from small gases (**Figure 2**). This explains the observed intensity differences and temperature shifts between mass loss and mass spectrometric data discussed above.

The corresponding EI mass spectra (**Figure S3**) were obtained by summation of the region of interest. With the above-mentioned restrictions of the SPI ionization threshold and the room-temperature sampling of the EI setup, as well as the help of structure databases, it can be concluded, that chemical bonded water (*m/z* 18) is released in the first pyrolysis step, and the fourth mass loss step belongs to the release of carbon dioxide (*m/z* 44). This behavior is not directly expected, as only LDPE (n C_2H_4) waste composed of carbon and hydrogen was inserted as feed material. There are several plausible paths of introducing oxygen to the system. The applied inert gas for the thermal analysis could have had oxygen impurities. To disprove this assumption, we tested the setup with pure carbon rods (**Figure S1**). The response of carbon dioxide was two orders of magnitude lower than the response in the coke measurements. Therefore, the carbon dioxide must be related to the plastic pyrolysis coke. We hypothesize that the release of carbon dioxide may result from the degradation products of common plasticiser. Evidence can be found in the soft photoionization mass spectra (**Figure 3**c). The mass spectrometric information of the four major mass loss steps possesses unique molecular information. The mass spectra in these regions of interest were summed, yielding four distinguished mass spectra over the range of 100-400 °C, 400-550 °C, 550-650 °C and 700-900 °C.

Starting with the temperature range of 100-400 °C, there is a huge difference between the chemical information revealed by the SPI and REMPI mass spectra. The highest signal (base peak) for the SPI spectrum is *m/z* 96 (tentatively heptadiene, C_7H_{12}) and a row of "triplets" ($[M]^{\bullet+}$, $[M+2]^{\bullet+}$, $[M+4]^{\bullet+}$) account for the majority of the signals. These "triplets" are caused by dienes, alkenes and alkanes differing in two hydrogen atoms (Δ*m/z* 2), whereas the homologue rows differ in chain length (CH_2, *m/z* 14).[6,21,29] In contrast, the REMPI spectrum features *m/z* 202 (pyrene, $C_{16}H_{10}$) as highest signal and there is a broad almost symmetric Gaussian distribution of signals tentatively attributed to other polycyclic aromatic hydrocarbons and alkylated homologue rows.

In the SPI spectrum, the broad pattern is a product of thermal cracking of the coke by random chain scission. [19] Therefore, the coke will most likely contain non or only partially pyrolyzed feed material, more specifically oligomeric structures consisting of long alkyl chains. In the lower mass range (*m/z* <

120) dienes are the most abundant signal in these “triplets”, followed by the respective alkene and alkane signals. The reason for the high diene contribution may that the smaller fragments are generated by multiple bond-breaking reactions. Moreover, this effect can be caused due to analyzing already pyrolyzed coke residue rather than the pure polymer feed shown in the majority of the literature. For larger molecules the alkene is favored, leading to alkenes giving the highest signal intensities, followed by alkanes and dienes. Also, a low contribution of aromatic species, such as benzene (*m/z* 78) and toluene (*m/z* 92) can be detected in the SPI spectra. For the focus on aromatic constituents, REMPI is far more sensitive and selective. A wide range primarily of polycyclic aromatic species can be observed with this method (**Figure 3**a, red). The high number of signals is a result of several effects: First, a variety of polycyclic aromatic substances like naphthalene (*m/z* 128), fluorene (*m/z* 166) or phenanthrene (*m/z* 178) with different degrees of alkylation is released from the coke. Second, oxygenated polycyclic aromatic species such as anthrone (*m/z* 194) are also present, overlapping with the signals of PAHs.

For structural validation of the observed species, another complementary technique is needed, namely pyrolysis gas chromatography with mass spectrometric detection (Pyr GCMS). (**Figure 4**). This technique allows approaching the isomeric complexity. It is reported that PAHs are common by-products of the formation of dienes and alkenes in pyrolysis reactors, depending on the deployed temperatures. [6]

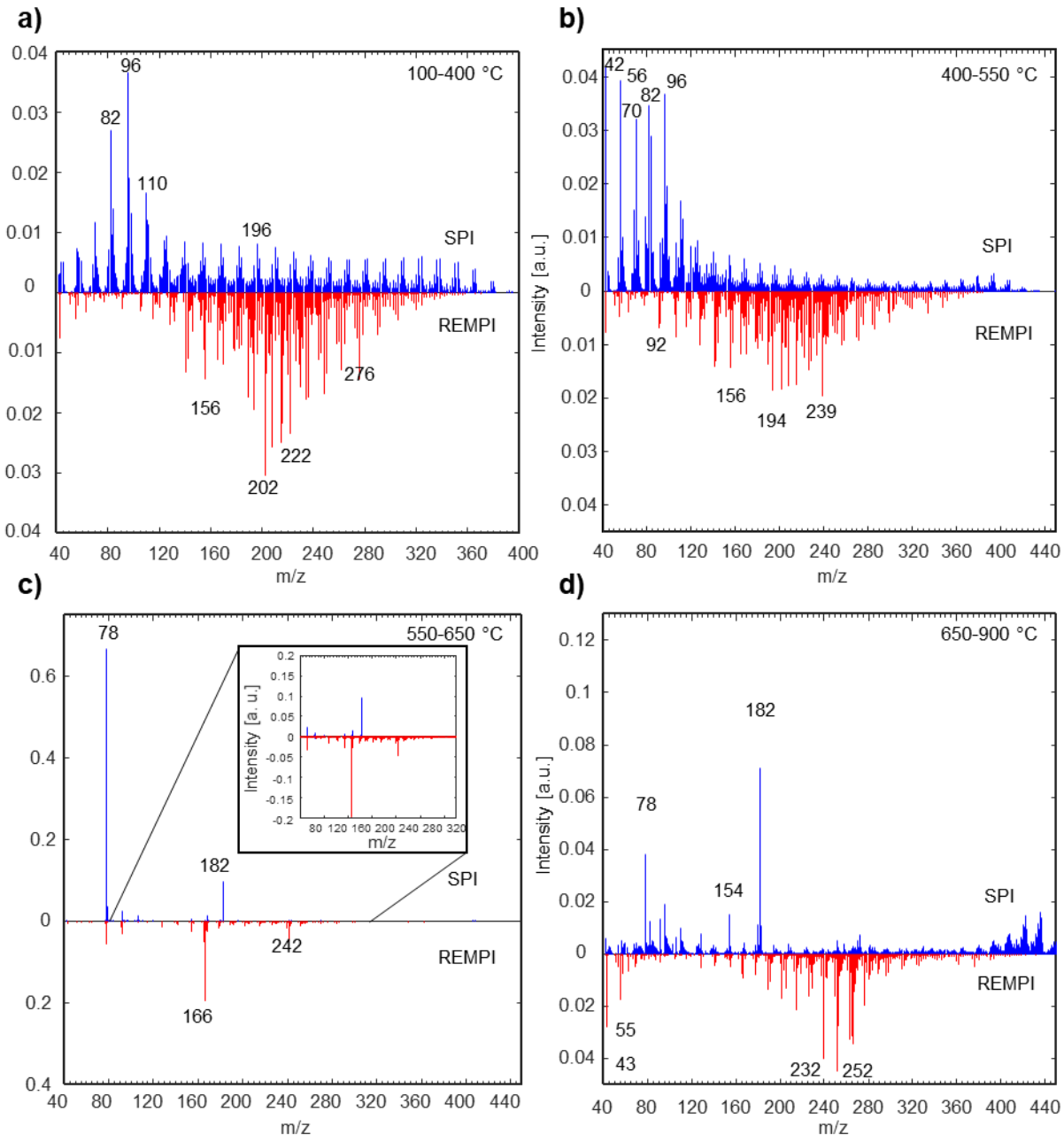

Figure 3. Overview of the TG-SPI/REMPI time-of-flight mass spectrometry results of Coke A; a) -d) "butterfly-plot" with average mass spectra (blue/up – SPI; red/down – REMPI) of the four different temperature mass loss events.

Consequently, the pyrolysis coke releases a substantial amount of material in secondary thermal treatment, even at comparable low temperatures below 400 °C. The evaporated material is primarily composed of water and a complex organic mixture dominated by alkanes, alkenes, and dienes. Critical for human health and the environment, a strong release of mutagenic and genotoxic PAHs was found and needs to be considered for disposal strategies. Nonetheless, regarding second usage and the

production of valuable products, these chemicals are highly demanded building blocks in the chemical industry and circular economy. [39]

For the temperature range of 400-550 °C, both ionization techniques show a clear shift towards lower *m/z* values (**Figure 3**b). As the temperatures rise, the kinetic of the bond breaking is increased and, thus, this is an expected observation. [6] The prior observed “triplets” are still found in the SPI spectrum but with much lower intensity than during the first release point, with *m/z* 42 (propene) being the base peak. In contrast, the maximum of the diene homolog row is again found at *m/z* 96, but as for the other dienes the intensities are reduced. At higher *m/z* values there is an increase in signal intensity, and a more abundant pattern between *m/z* 370-420 can be found. These larger and low volatile thermal analysis products are generated already at lower temperatures (**Figure 3**a) but reveal a slow release pattern combined with a certain proportion of tailing, classically observed for those heavier species. Another difference to the mass spectra of the first temperature range is the increase in intensity of monocyclic aromatics, primarily benzene (*m/z* 78) and toluene (*m/z* 92) as well as the occurrence of styrene (*m/z* 104) and methyl styrene (*m/z* 118). The rise in signal intensity of those small aromatic molecules supports the assessment that a second considerable pyrolysis of the coke residue takes place. A similar trend applies to the REMPI spectrum. Smaller aromatics can also be originated to a low extent from reaction processes of the alkanes, alkenes and dienes in the thermal balance. [40–42] Nonetheless, thermal analysis of pure PE samples with the same instrumental setup has not revealed any contribution of those aromatic constituents and, thus, they are predominantly released from the coke itself (**Figures S2**).

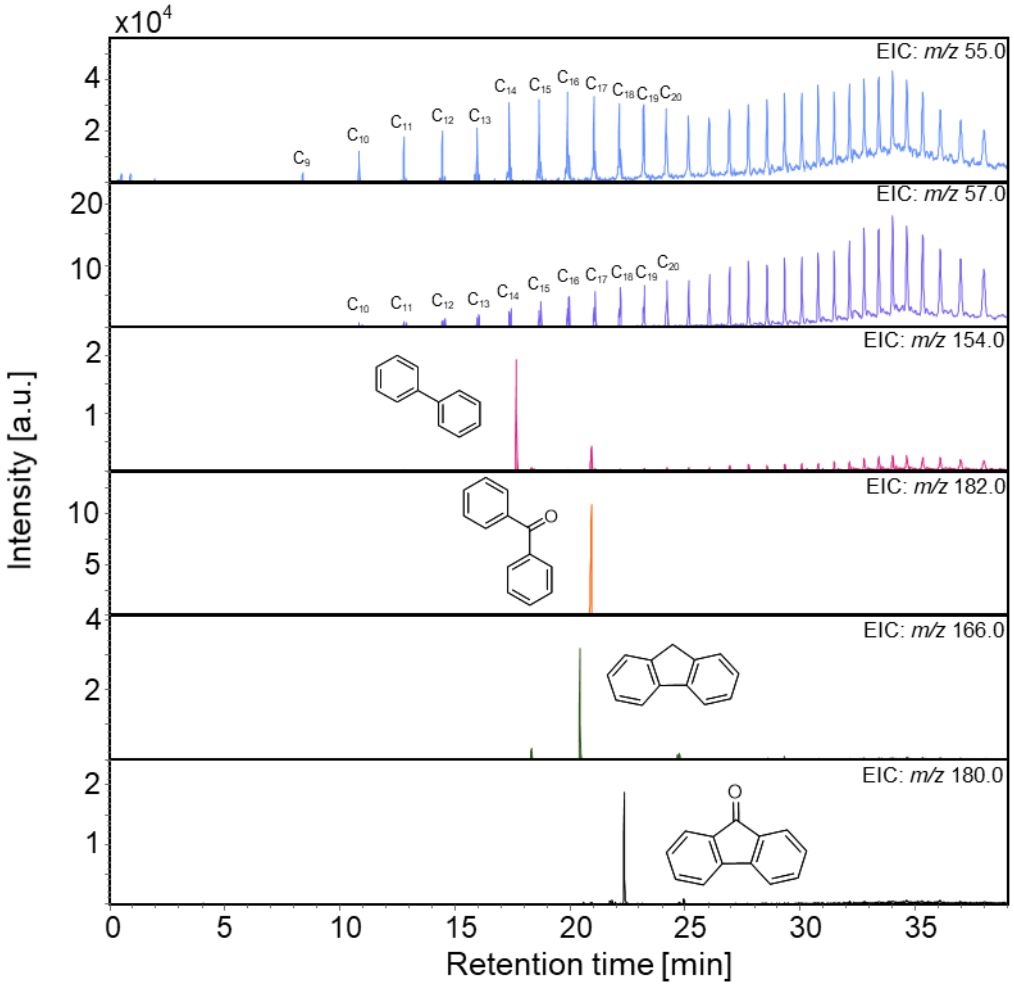

Figure 4. Pyrolysis GCMS results from Coke A of different characteristic extracted ion chromatograms with proposed structures based on the NIST database search. For alkanes and alkenes, a repetitive pattern of the homolog rows can be observed, whereas individual isomers for the PAHs and oxygenated PAHs, such as anthrone, can be found.

For the temperature range 550-650 °C, an entirely different behavior can be found (**Figure 3**c). The typical broad chemical pattern (**Figure 3**a/b) is not observed in the SPI and REMPI spectra and, in contrast, the spectrum is dominated by a few high-abundant signals. In the SPI spectrum, the signal of *m/z* 78 (benzene) is the most abundant signal, followed by *m/z* 182 (benzophenone) as the second most abundant signal, despite both having a rather poor ionization cross-section. [43] Other lower-abundant signals belong to toluene (*m/z* 92), xylene (*m/z* 106), biphenyl / ethynyl-naphthalene (m/z 154), and diphenylmethane (m/z 168). The latter can also be seen in the REMPI spectrum. Moreover, the REMPI spectrum shows an extremely high signal of fluorene (*m/z* 166) as well as benzene, toluene, and methyl-tetracene *(m/z* 242). Isomeric verification is based on a database comparison of the fragmentation pattern in the pyrolysis GCMS data set (**Figure 4**). The findings indicate a defined structure or single substance in the pyrolysis coke thermally degraded and released in a rather narrow temperature range of 550-650° C. This structure could be formed in the

pyrolysis reactor as a remnant that underwent incomplete pyrolysis pathways in the polymer waste recycling reactor due to inhomogeneous temperature distribution or low residence time. Despite the relatively low mass loss of this third step of approximately 5 w-%, the high contribution of individual chemicals needs to be considered. Functionalized molecules can be further used in chemical processing streams, but oxygenated PAHs are also reported to have a substantial carcinogenic and mutagenic effect. [44,45]

Benzophenone is a common additive in plastic packaging as an UV blocker to prevent photo-degradation of polymers, therefore commonly appearing in LDPE waste. [46,47] The strong UV absorption abilities [48] could also be the reason for the high signal intensity at *m/z* 182 in the SPI spectrum. In addition, some known products of fragmentation reactions like the loss of CO (*m/z* 154) or the loss of C_6H_5 (*m/z* 105) are observed. [49] Benzophenone is frequently used as a starter for radical polymerization processes. Consequently, it could non-intentionally act as a polymerization agent in the pyrolysis coke formation and be incorporated into the three-dimensional char network. This cross-linking is particularly described in the literature to be activated by UV radiation but also other triggering events. [50] This hypothesis would also explain the delayed release at elevated temperature at significantly higher temperature as the vapor pressure and boiling point of benzophenone could explain. At temperatures higher than 650 °C, no significant signals, not already observed at lower temperature, are observed in the mass spectra (**Figure 3**d). Hence, a thermal release of the already discussed molecular pattern is taking place with the release of carbon dioxide, as the most important step, lowering the residual mass substantially. In respect to lowering the disposal mass of residue coke from recycling processes, these high temperatures might be beneficial but have to be balanced against energy consumption. With a char formation potential of the pyrolysis reactor of several w-% and roughly 18 million tons of LDPE consumption annually in Europe, this multiplies to a million tons problem. Moreover, the second thermal treatment under pyrolytic conditions will give a purified highly aromatic carbonaceous material. These char materials are reported in literature for the usage in material science, such as for batteries, catalyst beds or water purification applications. [51,52]

Surprisingly, the evolved gas mixture from the thermal analysis of the coke exposed a high complexity. This finding was not directly expected, especially considering the pyrolytic waste recycling of pure LDPE feed. To address this aspect, thermal analysis high-resolution mass spectrometry was deployed to unravel the isobaric complexity. [30,53] With this, pure PAHs can be directly distinguished from oxygenated PAHs with the same nominal mass, and the high mass accuracy allowed for direct attribution of the elemental composition as another validation for the chemical discussion above. A broad mass range up to *m/z* 600 was found (**Figure 5**a/b), and more than 600 sum formulae could be attributed. Only two major compound classes were identified, with a relative intensity of roughly 90 % for the CH-class and 8% for the CHO_1-class (**Figure S4**). These findings are in agreement with the results

of the TA-PIMS measurements and the expected major products of the not oxygen-containing polymeric feed. The oxygenated compounds of the CHO_1-class are caused by the plasticizer degradation products or thermal residues of other additives. **Figure 5**a displays the result for sample A as a survey plot. In this three-dimensional representation of *m/z* versus temperature, three events occur until 600 °C. The intensities are different between the SPI/REMPI-setup and the FT-ICR results, mainly caused by different ionization schemes, FT-ICR using atmospheric pressure photoionization, and the specific mass spectrometric techniques. Here, in the temperature range of 300-450 °C, a lower response is detected in contrast to the first mass loss step at 200-300 °C. **Figure 5**b shows the averaged mass spectra along the complete temperature range and the different isobars can be clearly separated (S6). It has to be noted, the instrumental setup was optimized for a mass range between *m/z* 150 and *m/z* 1000; therefore small pyrolysis products are not detected, and a focus towards the heavier compounds is achieved.

Figure 5c displays the carbon number versus double bond equivalent (DBE) diagram for the CH-class. Utilizing the DBE, a measure for the unsaturation of a molecule, aromatic structures can be discussed. [54] Two molecular distributions can be observed, with the first distribution (**Figure 5**c, yellow) exhibiting rather low DBE values (1-6) and a broad carbon number spread (#C 12-41) and the second pattern (**Figure 5**c, green) closely located to the planar aromatic limit with high DBE values (12-22) and a narrower carbon number spread (3-7 #C width). The first pattern accounts for the alkenes (DBE 1), dienes (DBE 2), benzene- (DBE 4), and naphthenic-derivatives (DBE 2-5) in detail discussed above and additionally validated here using the exact mass measurement. More interestingly, the second pattern accounts for polycyclic aromatic hydrocarbons. In this respect, the planar aromatic limit is a conceptual border for polycyclic aromatic carbons with the highest possible unsaturation in the naturally occurring chemical space. The location of a majority of the second distribution close to this line allows hypothesizing highly condensed aromatic cores with a low degree of alkylation or naphthenic contribution. Despite the almost absent contribution of heteroelements, such as nitrogen and sulphur, the pyrolysis chars can be compared to asphaltenes, a highly aromatic and complex fraction of petroleum. Two molecular architecture models are discussed in asphaltene science: Large condensed aromatic structures (island motif) and smaller aromatic cores bridged by linkers (archipelago motif). Comparison to prior investigations of asphaltenes by the thermal analysis setup let us hypothesize a certain contribution of both motifs. Purified asphaltenes also revealed the characteristic “gap” between two distributions in the carbon number versus DBE visualization. Archipelago-type char will decompose at elevated temperatures into the second distribution found close to the planar aromatic limit. Consequently, the plastic pyrolysis coke still revealed a significant contribution of pyrolyzable material belonging to the archipelago motif as a pyrolytic precursor to more condensed island motifs or even fully graphitized char. [54]

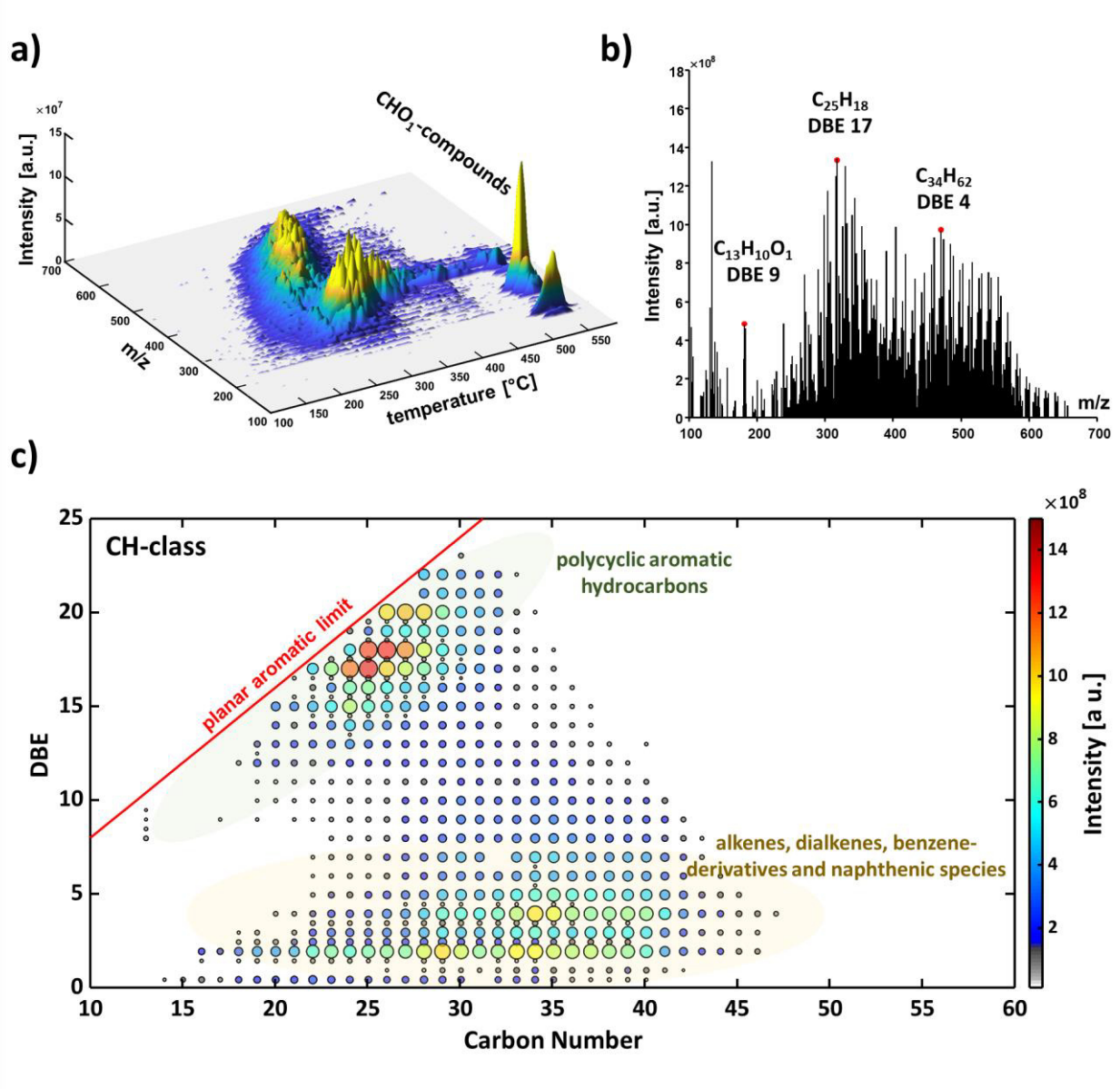

Figure 5. Compilation of the results from the thermal analysis ultrahigh-resolution mass spectrometric coke analysis (TG FT-ICR MS) of Coke A. a) Survey data visualization of the general mass spectrometric response (temperature versus m/z). b) Average mass spectrum of the attributed elemental compositions. c) Double bond equivalent (DBE) versus carbon number (#C) diagram of the CH-class. Two distinct chemical distributions, one at higher DBE values with comparable low #C spread and second at low DBE 0-5 with a high #C spread, attributed to polycyclic aromatic hydrocarbons and alkenes, dienes, benzene-derivatives, and naphthenic species, can be found, respectively.

Conclusion

Thermal analysis of coke from recycled plastic waste was investigated the first time by deploying a second thermal treatment with comprehensive evolved gas analysis. It was found that the residual mass of the coke can further be reduced by a factor of two with a residual mass of 40-55 w-%, significantly lowering the amount of material for disposal but also removing potential toxic and environmentally harmful compounds. This forms the basis of a concept strongly to be evaluated with the required energetic demand in future studies.

Interestingly, the thermal treatment revealed four distinct mass loss steps, with the highest occurring at 900 °C. The evolved gas mixture could successfully be described by different mass spectrometric analysis platforms. Common harsh electron ionization allowed to attribute the loss of carbon dioxide as well as residual water. The release of carbon dioxide accounts for at least 10 w-% attributed to the pyrolysis products of plasticizers and other additives. Soft ionization schemes, such as SPI and REMPI, revealed a complex hydrocarbon pattern, primarily composed of dienes, alkenes and alkanes, but also polycyclic aromatic hydrocarbons and their alkylated derivatives have been detected. Interestingly, the common plastic UV-absorber benzophenone was identified with different methods at temperatures above 550 °C. This delayed release is explained by the incorporation into the three-dimensional char network only decomposed at elevated temperatures. Finally, high-resolution mass spectrometry allowed to unravel the complex pattern on the isobaric level and indications for a three-dimensional network composed of archipelago and island structural motifs were found, highlighting the not-fully graphitized and heterogeneous character of the chars.

On the one hand, from an economic point of view, the high content of released alkenes and dienes, and other building blocks, such as benzene and toluene, could be further utilized in the chemical industry. On the other hand, those compounds need to be considered in terms of human health and ecological toxicology for disposal strategies to the environment. Furthermore, we hypothesize that the residual from the second thermal treatment can be used to produce active carbon materials utilized in battery research, catalysis science or water purification. [51,52] Future studies will focus on the description of pyrolysis chars generated under different pyrolytic conditions or from other plastic waste types. Particularly, also morphological aspects will be investigated by microscopy, allowing to develop efficient utilization strategies for these solid waste recycling residues in a circular economy.

Acknowledgement

Funding by the Horizon 2020 program for the EU FT-ICR MS project (European Network of Fourier-Transform Ion-Cyclotron-Resonance Mass Spectrometry Centers, Grant agreement ID: 731077) and for the regional development project (TBI-V-1 -262-VBW-093) is gratefully acknowledged. The authors thank the German Research Foundation (DFG) for funding of the Bruker FT-ICR MS (INST 264/56). Special thanks to the HITACHI company for providing us the thermal analyser and for TotalEnergies, Belgium for kindly providing us the interesting sample material.

Associated Content

Supporting Information

The Supporting Information is available free of charge at XXX. Tabular information about the applied process parameters (**Table S1**), tabular information about the pyrolysis gas chromatographic results (**Table S2**), Total ion count versus temperature for the empty crucible and pure carbon rods (**Figure S1**), results of the thermal analysis of pure polyethylene sample with REMPI (**Figure S3**), compound class distribution of the high-resolution mass spectrometric analysis **(Figure S4**), Kendrick mass defect plot of the thermal analysis FT-ICR MS (**Figure S5**), and visualization of the isobaric complexity by enlargement of a nominal mass (**Figure S6**).

References

[1] S. Mossman, Plastics and Social Responsibility, in: S. Lambert (Ed.), Provocative Plastics: Their Value in Design and Material Culture, Springer International Publishing, Cham, 2020, pp. 275–295.

[2] K. Pivnenko, M.K. Eriksen, J.A. Martín-Fernández, E. Eriksson, T.F. Astrup, Recycling of plastic waste: Presence of phthalates in plastics from households and industry, Waste management (New York, N.Y.) 54 (2016) 44–52. https://doi.org/10.1016/j.wasman.2016.05.014.

[3] A. Tullo, Europe is implementing a tax on plastic, C&EN Global Enterp 99 (2021) 34. https://doi.org/10.1021/cen-09902-cover7.

[4] M.S. Qureshi, A. Oasmaa, H. Pihkola, I. Deviatkin, A. Tenhunen, J. Mannila, H. Minkkinen, M. Pohjakallio, J. Laine-Ylijoki, Pyrolysis of plastic waste: Opportunities and challenges, Journal of Analytical and Applied Pyrolysis (2020) 104804. https://doi.org/10.1016/j.jaap.2020.104804.

[5] S.D. Anuar Sharuddin, F. Abnisa, W.M.A. Wan Daud, M.K. Aroua, A review on pyrolysis of plastic wastes, Energy Conversion and Management 115 (2016) 308–326. https://doi.org/10.1016/j.enconman.2016.02.037.

[6] S.-H. Jung, M.-H. Cho, B.-S. Kang, J.-S. Kim, Pyrolysis of a fraction of waste polypropylene and polyethylene for the recovery of BTX aromatics using a fluidized bed reactor, Fuel Processing Technology 91 (2010) 277–284. https://doi.org/10.1016/j.fuproc.2009.10.009.

[7] W.M. Lewandowski, K. Januszewicz, W. Kosakowski, Efficiency and proportions of waste tyre pyrolysis products depending on the reactor type—A review, Journal of Analytical and Applied Pyrolysis 140 (2019) 25–53. https://doi.org/10.1016/j.jaap.2019.03.018.

[8] U. Hujuri, A.K. Ghoshal, S. Gumma, Modeling pyrolysis kinetics of plastic mixtures, Polymer Degradation and Stability 93 (2008) 1832–1837. https://doi.org/10.1016/j.polymdegradstab.2008.07.006.

[9] A.O. Oyedun, T. Gebreegziabher, D.K. Ng, C.W. Hui, Mixed-waste pyrolysis of biomass and plastics waste – A modelling approach to reduce energy usage, Energy 75 (2014) 127–135. https://doi.org/10.1016/j.energy.2014.05.063.

[10] S.S. Park, D.K. Seo, S.H. Lee, T.-U. Yu, J. Hwang, Study on pyrolysis characteristics of refuse plastic fuel using lab-scale tube furnace and thermogravimetric analysis reactor, Journal of Analytical and Applied Pyrolysis 97 (2012) 29–38. https://doi.org/10.1016/j.jaap.2012.06.009.

[11] A. Dhahak, C. Grimmer, A. Neumann, C. Rüger, M. Sklorz, T. Streibel, R. Zimmermann, G. Mauviel, V. Burkle-Vitzthum, Real time monitoring of slow pyrolysis of polyethylene terephthalate (PET) by different mass spectrometric techniques, Waste management (New York, N.Y.) 106 (2020) 226–239. https://doi.org/10.1016/j.wasman.2020.03.028.

[12] Y. Yu, Y. Yang, Z. Cheng, P.H. Blanco, R. Liu, A.V. Bridgwater, J. Cai, Pyrolysis of Rice Husk and Corn Stalk in Auger Reactor. 1. Characterization of Char and Gas at Various Temperatures, Energy Fuels 30 (2016) 10568–10574. https://doi.org/10.1021/acs.energyfuels.6b02276.

[13] N. Mahinpey, P. Murugan, T. Mani, R. Raina, Analysis of Bio-Oil, Biogas, and Biochar from Pressurized Pyrolysis of Wheat Straw Using a Tubular Reactor, Energy Fuels 23 (2009) 2736–2742. https://doi.org/10.1021/ef8010959.

[14] J. Hertzog, V. Carré, Y. Le Brech, A. Dufour, F. Aubriet, Toward Controlled Ionization Conditions for ESI-FT-ICR-MS Analysis of Bio-Oils from Lignocellulosic Material, Energy Fuels 30 (2016) 5729–5739. https://doi.org/10.1021/acs.energyfuels.6b00655.

[15] P.T. Williams, E.A. Williams, Interaction of Plastics in Mixed-Plastics Pyrolysis, Energy Fuels 13 (1999) 188–196. https://doi.org/10.1021/ef980163x.

[16] A. López, I. de Marco, B.M. Caballero, M.F. Laresgoiti, A. Adrados, A. Torres, Pyrolysis of municipal plastic wastes II: Influence of raw material composition under catalytic conditions,

Waste management (New York, N.Y.) 31 (2011) 1973–1983. https://doi.org/10.1016/j.wasman.2011.05.021.
[17] V. Cozzani, Characterization of Coke Formed in the Pyrolysis of Polyethylene, Ind. Eng. Chem. Res. 36 (1997) 5090–5095. https://doi.org/10.1021/ie970381y.
[18] J. Jamradloedluk, C. Lertsatitthanakorn, Characterization and Utilization of Char Derived from Fast Pyrolysis of Plastic Wastes, Procedia Engineering 69 (2014) 1437–1442. https://doi.org/10.1016/j.proeng.2014.03.139.
[19] İ. Çit, A. Sınağ, T. Yumak, S. Uçar, Z. Mısırlıoğlu, M. Canel, Comparative pyrolysis of polyolefins (PP and LDPE) and PET, Polym. Bull. 64 (2010) 817–834. https://doi.org/10.1007/s00289-009-0225-x.
[20] P.T. Williams, E.A. Williams, Fluidised bed pyrolysis of low density polyethylene to produce petrochemical feedstock, Journal of Analytical and Applied Pyrolysis 51 (1999) 107–126. https://doi.org/10.1016/S0165-2370(99)00011-X.
[21] D.S. Achilias, C. Roupakias, P. Megalokonomos, A.A. Lappas, E.V. Antonakou, Chemical recycling of plastic wastes made from polyethylene (LDPE and HDPE) and polypropylene (PP), Journal of Hazardous Materials 149 (2007) 536–542. https://doi.org/10.1016/j.jhazmat.2007.06.076.
[22] T. Streibel, R. Geißler, M. Saraji-Bozorgzad, M. Sklorz, E. Kaisersberger, T. Denner, R. Zimmermann, Evolved gas analysis (EGA) in TG and DSC with single photon ionisation mass spectrometry (SPI-MS): molecular organic signatures from pyrolysis of soft and hard wood, coal, crude oil and ABS polymer, J Therm Anal Calorim 96 (2009) 795–804. https://doi.org/10.1007/s10973-009-0035-2.
[23] T. Streibel, R. Zimmermann, Resonance-enhanced multiphoton ionization mass spectrometry (REMPI-MS): applications for process analysis, Annual review of analytical chemistry (Palo Alto, Calif.) 7 (2014) 361–381. https://doi.org/10.1146/annurev-anchem-062012-092648.
[24] P.T. Williams, P.A. Horne, D.T. Taylor, Polycyclic aromatic hydrocarbons in polystyrene derived pyrolysis oil, Journal of Analytical and Applied Pyrolysis 25 (1993) 325–334. https://doi.org/10.1016/0165-2370(93)80052-2.
[25] C. Peniche-Covas, M.S. Jiménez, A. Núñez, Characterization of silver-binding chitosan by thermal analysis and electron impact mass spectrometry, Carbohydrate Polymers 9 (1988) 249–256. https://doi.org/10.1016/0144-8617(88)90043-4.
[26] Y.F. Huang, W.H. Kuan, P.T. Chiueh, S.L. Lo, Pyrolysis of biomass by thermal analysis-mass spectrometry (TA-MS), Bioresource technology 102 (2011) 3527–3534. https://doi.org/10.1016/j.biortech.2010.11.049.
[27] H. Yan, F. Mao, J. Wang, Thermogravimetric-mass spectrometric characterization of thermal decomposition of lignite with attention to the evolutions of small molecular weight oxygenates, Journal of Analytical and Applied Pyrolysis 146 (2020) 104781. https://doi.org/10.1016/j.jaap.2020.104781.
[28] C.P. Rüger, C. Grimmer, M. Sklorz, A. Neumann, T. Streibel, R. Zimmermann, Combination of Different Thermal Analysis Methods Coupled to Mass Spectrometry for the Analysis of Asphaltenes and Their Parent Crude Oils: Comprehensive Characterization of the Molecular Pyrolysis Pattern, Energy Fuels 32 (2018) 2699–2711. https://doi.org/10.1021/acs.energyfuels.7b02762.
[29] C. Grimmer, L. Friederici, T. Streibel, A. Naim, V. Cirriez, P. Giusti, C. Afonso, C.P. Rüger, R. Zimmermann, Characterization of Polyethylene Branching by Thermal Analysis-Photoionization Mass Spectrometry, Journal of the American Society for Mass Spectrometry 31 (2020) 2362–2369. https://doi.org/10.1021/jasms.0c00291.
[30] C.P. Rüger, T. Miersch, T. Schwemer, M. Sklorz, R. Zimmermann, Hyphenation of Thermal Analysis to Ultrahigh-Resolution Mass Spectrometry (Fourier Transform Ion Cyclotron Resonance Mass Spectrometry) Using Atmospheric Pressure Chemical Ionization For Studying

Composition and Thermal Degradation of Complex Materials, Analytical chemistry 87 (2015) 6493–6499. https://doi.org/10.1021/acs.analchem.5b00785.

[31] D. Brecht, F. Uteschil, O.J. Schmitz, Thermogravimetry coupled to an atmospheric pressure photo ionization quadrupole mass spectrometry for the product control of pharmaceutical formulations and the analysis of plasticizers in polymers, Talanta 198 (2019) 440–446. https://doi.org/10.1016/j.talanta.2019.01.118.

[32] S. Otto, T. Streibel, S. Erdmann, M. Sklorz, D. Schulz-Bull, R. Zimmermann, Application of pyrolysis–mass spectrometry and pyrolysis–gas chromatography–mass spectrometry with electron-ionization or resonance-enhanced-multi-photon ionization for characterization of crude oils, Analytica chimica acta 855 (2015) 60–69. https://doi.org/10.1016/J.ACA.2014.11.030.

[33] N. Regnier, B. Mortaigne, Analysis by pyrolysis/gas chromatography/mass spectrometry of glass fibre/vinylester thermal degradation products, Polymer Degradation and Stability 49 (1995) 419–428. https://doi.org/10.1016/0141-3910(95)00129-A.

[34] M.C.A.N. Analytical, Using the Grubbs and Cochran tests to identify outliers, Analytical methods advancing methods and applications 7 (2015) 7948–7950. https://doi.org/10.1039/C5AY90053K.

[35] K. Seki, Ionization Energies of Free Molecules and Molecular Solids, Molecular Crystals and Liquid Crystals Incorporating Nonlinear Optics 171 (1989) 255–270. https://doi.org/10.1080/00268948908065800.

[36] M. Saraji-Bozorgzad, R. Geißler, T. Streibel, M. Sklorz, E. Kaisersberger, T. Denner, R. Zimmermann, Hyphenation of a thermobalance to soft single photon ionisation mass spectrometry for evolved gas analysis in thermogravimetry (TG-EGA), J Therm Anal Calorim 97 (2009) 689–694. https://doi.org/10.1007/s10973-009-0069-5.

[37] M.R. Saraji-Bozorgzad, T. Streibel, E. Kaisersberger, T. Denner, R. Zimmermann, Detection of organic products of polymer pyrolysis by thermogravimetry-supersonic jet-skimmer time-of-flight mass spectrometry (TG-Skimmer-SPI-TOFMS) using an electron beam pumped rare gas excimer VUV-light source (EBEL) for soft photo ionisation, J Therm Anal Calorim 105 (2011) 691–697. https://doi.org/10.1007/s10973-011-1383-2.

[38] J.L. Bredas, R. Silbey, D.S. Boudreaux, R.R. Chance, Chain-length dependence of electronic and electrochemical properties of conjugated systems: polyacetylene, polyphenylene, polythiophene, and polypyrrole, J. Am. Chem. Soc. 105 (1983) 6555–6559. https://doi.org/10.1021/ja00360a004.

[39] M.N. Siddiqui, Conversion of hazardous plastic wastes into useful chemical products, Journal of Hazardous Materials 167 (2009) 728–735. https://doi.org/10.1016/j.jhazmat.2009.01.042.

[40] J.M. Andrésen, J.J. Strohm, L. Sun, C. Song, Relationship between the Formation of Aromatic Compounds and Solid Deposition during Thermal Degradation of Jet Fuels in the Pyrolytic Regime, Energy Fuels 15 (2001) 714–723. https://doi.org/10.1021/ef000256q.

[41] F.-D. Kopinke, B. Ondruschka, G. Zimmermann, J. Dermietzel, Rearrangement reactions in the thermal formation of aromatics from cycloolefins. 14C-labelling studies, Journal of Analytical and Applied Pyrolysis 13 (1988) 259–275. https://doi.org/10.1016/0165-2370(88)80011-1.

[42] X. Qin, H. Chi, W. Fang, Y. Guo, L. Xu, Thermal stability characterization of n-alkanes from determination of produced aromatics, Journal of Analytical and Applied Pyrolysis 104 (2013) 593–602. https://doi.org/10.1016/j.jaap.2013.05.009.

[43] T. Adam, R. Zimmermann, Determination of single photon ionization cross sections for quantitative analysis of complex organic mixtures, Analytical and bioanalytical chemistry 389 (2007) 1941–1951. https://doi.org/10.1007/s00216-007-1571-x.

[44] A.L. Knecht, B.C. Goodale, L. Truong, M.T. Simonich, A.J. Swanson, M.M. Matzke, K.A. Anderson, K.M. Waters, R.L. Tanguay, Comparative developmental toxicity of environmentally relevant

oxygenated PAHs, Toxicology and applied pharmacology 271 (2013) 266–275. https://doi.org/10.1016/j.taap.2013.05.006.

[45] S. Lundstedt, P.A. White, C.L. Lemieux, K.D. Lynes, I.B. Lambert, L. Öberg, P. Haglund, M. Tysklind, Sources, Fate, and Toxic Hazards of Oxygenated Polycyclic Aromatic Hydrocarbons (PAHs) at PAH- contaminated Sites, AMBIO: A Journal of the Human Environment 36 (2007) 475–485. https://doi.org/10.1579/0044-7447(2007)36[475:SFATHO]2.0.CO;2.

[46] H. Jia, H. Wang, W. Chen, The combination effect of hindered amine light stabilizers with UV absorbers on the radiation resistance of polypropylene, Radiation Physics and Chemistry 76 (2007) 1179–1188. https://doi.org/10.1016/j.radphyschem.2006.12.008.

[47] J. Zakrzewski, J. Szymanowski, 2-Hydroxybenzophenone UV-absorbers containing 2,2,6,6-tetramethylpiperidine (HALS) group — benzoylation of corresponding phenol derivatives, Polymer Degradation and Stability 67 (2000) 279–283. https://doi.org/10.1016/S0141-3910(99)00126-3.

[48] Z. Gouid, A. Röder, B.K. Cunha de Miranda, M.-A. Gaveau, M. Briant, B. Soep, J.-M. Mestdagh, M. Hochlaf, L. Poisson, Energetics and ionization dynamics of two diarylketone molecules: benzophenone and fluorenone, Phys. Chem. Chem. Phys. 21 (2019) 14453–14464. https://doi.org/10.1039/C9CP02385B.

[49] D. Srzić, S. Martinović, P. Vujanić, Z. Meić, Randomization in the fragmentation of benzophenone, Rapid Commun. Mass Spectrom. 7 (1993) 163–166. https://doi.org/10.1002/rcm.1290070210.

[50] B. Qu, Y. Xu, L. Ding, B. Rnby, A new mechanism of benzophenone photoreduction in photoinitiated crosslinking of polyethylene and its model compounds, J. Polym. Sci. A Polym. Chem. 38 (2000) 999–1005. https://doi.org/10.1002/(SICI)1099-0518(20000315)38:6<999:AID-POLA9>3.0.CO;2-1.

[51] J. Xu, Y. Zhang, Z. Huang, C. Jia, S. Wang, Surface Modification of Carbon-Based Electrodes for Vanadium Redox Flow Batteries, Energy Fuels. https://doi.org/10.1021/acs.energyfuels.1c00722.

[52] P.S. Veluri, N. Katchala, S. Anandan, M. Pramanik, K. NarayanSrinivasan, B. Ravi, T. N. Rao, Petroleum Coke as an Efficient Single Carbon Source for High-Energy and High-Power Lithium-Ion Capacitors, Energy Fuels. https://doi.org/10.1021/acs.energyfuels.1c00665.

[53] Robb, Covey, Bruins, Atmospheric pressure photoionization: an ionization method for liquid chromatography-mass spectrometry, Anal. Chem. 72 (2000) 3653–3659. https://doi.org/10.1021/ac0001636.

[54] A. Neumann, M.L. Chacón-Patiño, R.P. Rodgers, C.P. Rüger, R. Zimmermann, Investigation of Island/Single-Core- and Archipelago/Multicore-Enriched Asphaltenes and Their Solubility Fractions by Thermal Analysis Coupled with High-Resolution Fourier Transform Ion Cyclotron Resonance Mass Spectrometry, Energy Fuels 35 (2021) 3808–3824. https://doi.org/10.1021/acs.energyfuels.0c03751.

Comprehensive chemical description of pyrolysis chars from low-density polyethylene (LDPE) by thermal analysis hyphenated to different mass spectrometric approaches

Lukas Friederici[1,2], Eric Schneider[1,2], Gaëtan Burnens[3,4], Thorsten Streibel[1,5], Pierre Giusti[4,6], Christopher P. Rüger*[1,2,4], Ralf Zimmermann[1,2,5]

1 –Joint Mass Spectrometry Centre (JMSC)/Chair of Analytical Chemistry, University of Rostock, 18059 Rostock, Germany

2 – Department Life, Light & Matter (LLM), University of Rostock, 18051 Rostock, Germany

3 – TotalEnergies, Total Research and Technology Feluy (TRTF), B-7181 Feluy, Belgium

4 – International Joint Laboratory−iC2MC: Complex Matrices Molecular Characterization, TotalEnergies - TRTG Refining and Chemicals, Gonfreville l'Orcher, 76700 Harfleur, France

5 – Joint Mass Spectrometry Centre (JMSC)/Helmholtz Zentrum München, Comprehensive Molecular Analytics, 85764 Neuherberg, Germany

6 – TotalEnergies, TRTG Refining and Chemicals, Gonfreville l'Orcher, 76700 Harfleur, France

* – corresponding author, christopher.rueger@uni-rostock.de

Keywords

pyrolysis, recycling, coke, thermal analysis, mass spectrometry, polyethylene

Table of Content

Table S3. Detailed description of the applied process parameters.

#	sample name	mass LDPE [kg]	reactor exit temperature [°C]	mixing speed [rpm]	purge gas	mass flow [kg/h]
1	Coke A	20	260-280	80	Nitrogen	~2.7
2	Coke B	18.9	250-270	50	Argon	1.7-2.3
3	Coke C	20.0	270-290	80	Argon, continuous flow 120 ml/min	2.4-2.6
4	Coke D	18.6	260-295	80	Nitrogen, continuous flow 120 ml/min	2.6
5	Coke E	22.5	310-330	160	Nitrogen	~3-5

Table S4. Pyr GC EIQMS results from sample A. Identified species assigned with the NIST Library and a match about 90 %.

#	identified substance	*m/z*	retention time [min]	#	identified substance	*m/z*	retention time [min]
1	Nonene	126	8.41	**17**	Hexadecane	226	19.97
2	Decene	140	10.87	**18**	Fluorene	166	20.45
3	Decane	142	11.01	**19**	Benzophenone	182	20.95
4	Undecene	154	12.81	**20**	Heptadecene	238	21.07
5	Undecane	156	12.94	**21**	Heptadecane	240	21.12
6	Dodecene	168	14.49	**22**	Octadecene	252	22.18
7	Dodecane	170	14.59	**23**	Octadecane	254	22.21
8	Tridecene	182	15.99	**24**	9H-Fluoren-9-one	180	22.38
9	Tridecane	184	16.08	**25**	Phenanthren	178	22.96
10	Tetradecene	196	17.39	**26**	Nonadecene	266	23.2
11	Tetradecane	198	17.47	**27**	Nonadecane	268	23.26
12	Biphenyl	154	17.7	**28**	Icosene	280	24.25
13	Biphenylmethane	168	18.34	**29**	Icosane	282	24.69
14	Pentadecene	210	18.69	**30**	Anthrone	194	24.69
15	Pentadecane	212	18.76	**31**	Triphenylmethane	244	24.77
16	Hexadecene	224	19.92	**32**	9-Phenyl-9H-Fluorene	242	26.26

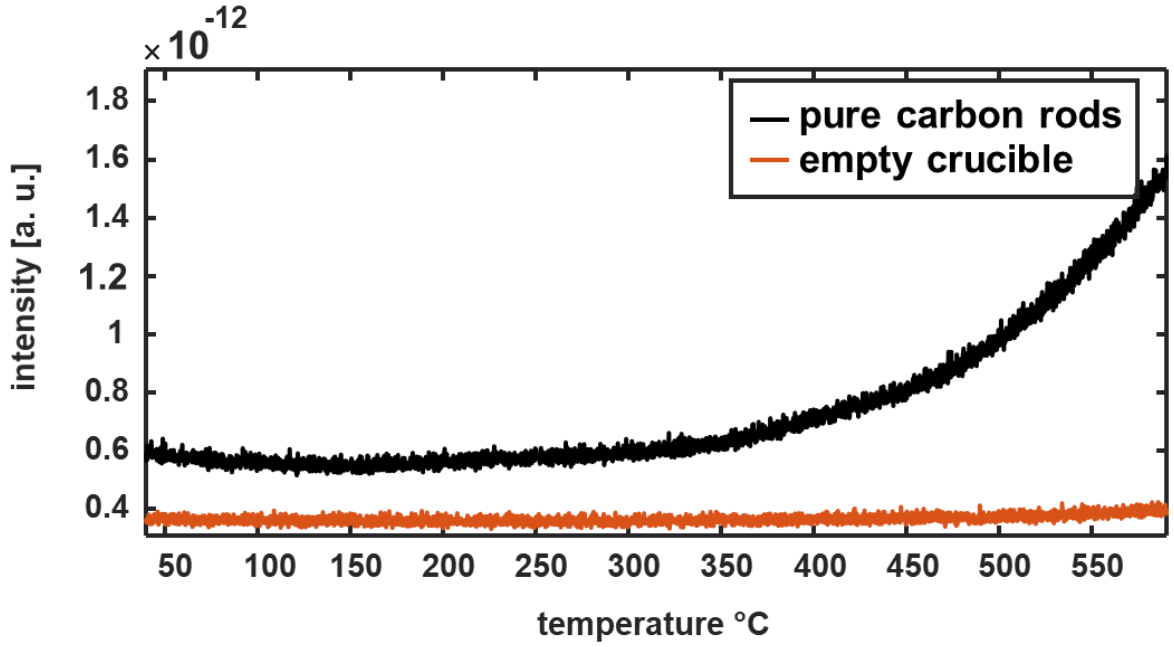

Figure S7. Analysis of light gases and small molecules by hyphenation of TG and QMS. Test of the setup with pure carbon rods and an empty crucible. The temperature resolved total ion chromatogram show a steady increase in signal intensity for the carbon rods, which may be belongs to remaining oxygen in the gas supply.

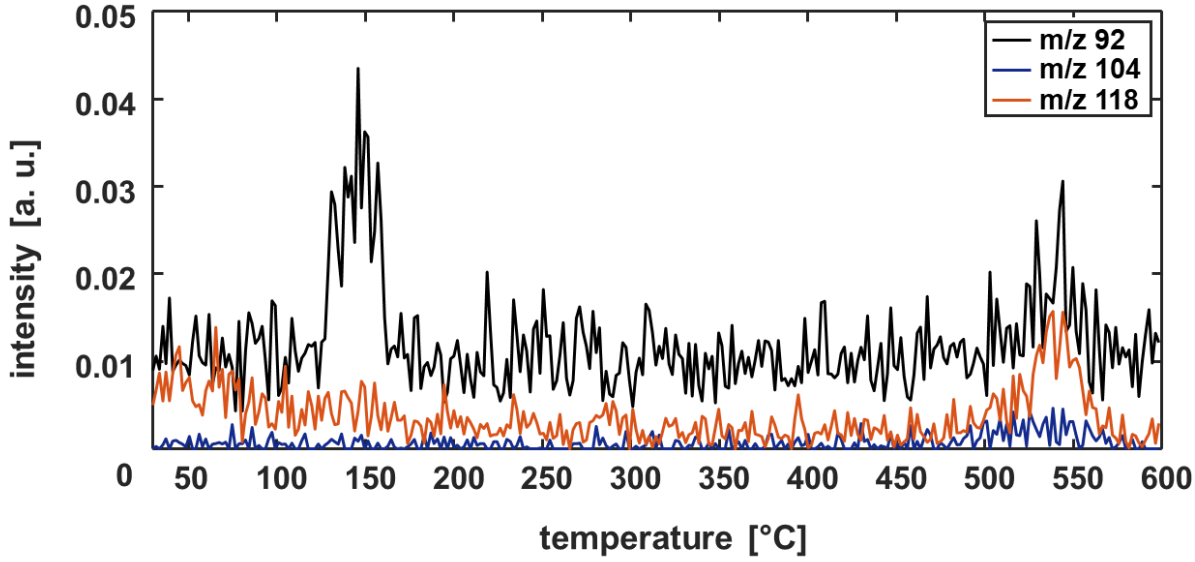

Figure S8. Thermal analysis of pure PE samples with the TG-PIMS setup with REMPI for small aromatic structures. Therefore, selected ion chromatograms are depicted.

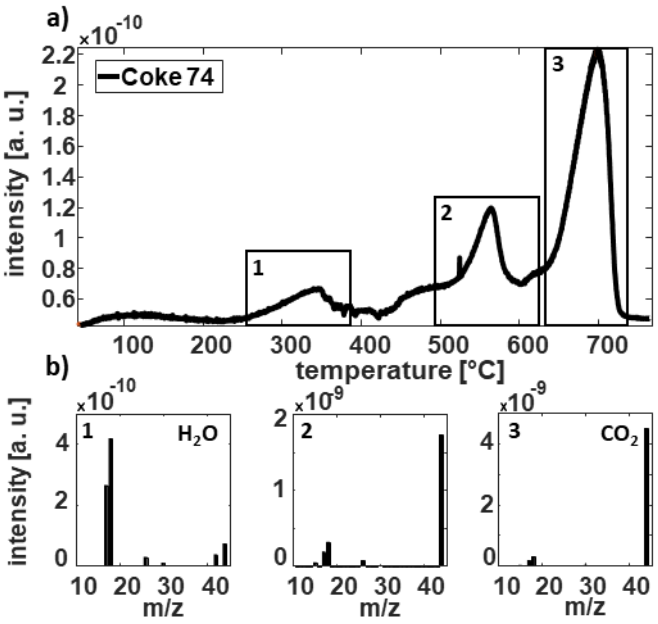

Figure S9. Small molecule analysis results of the hyphenation of TG-QMS. The temperature resolved total ion chromatogram (a) shows three different events. This correspond to the generation of water (1) and carbon dioxide (2, 3) (b).

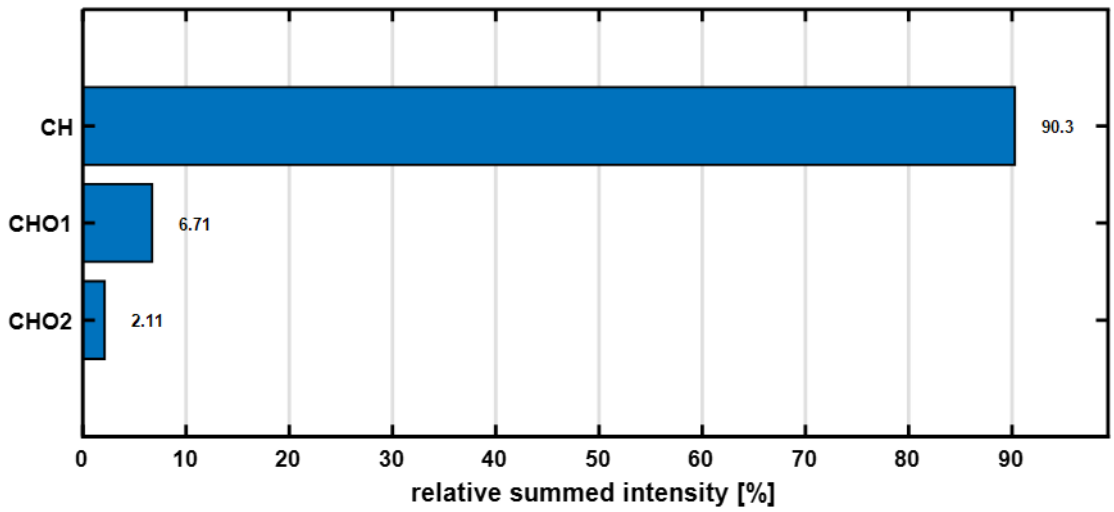

Figure S10. Compound class distribution assigned with the TG-(+)APPI-FT-ICR MS of sample A.

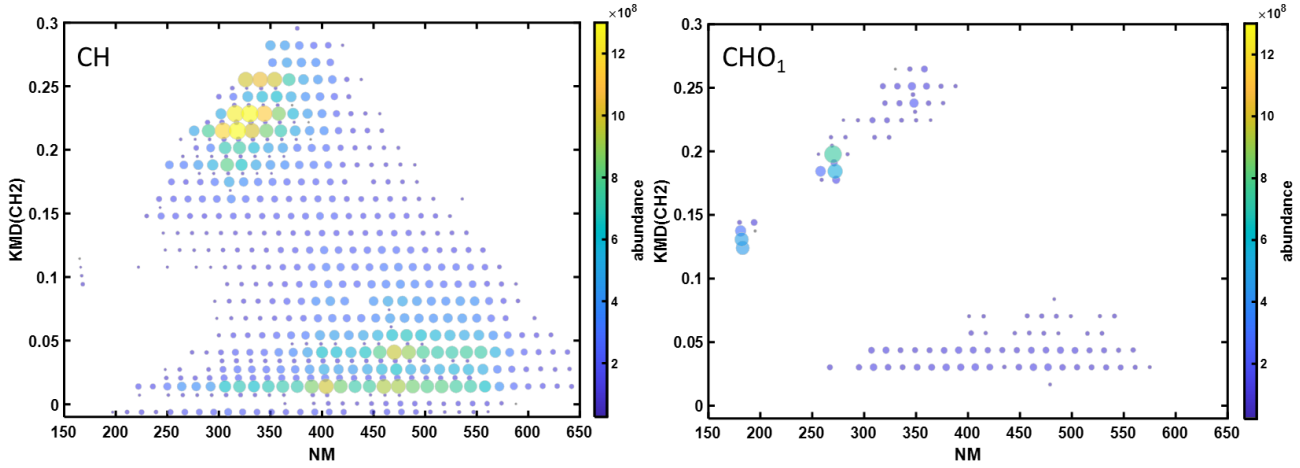

Figure S11. Kendrick mass defect determined with the exact molecular mass. On the horizontal axes the chemical compound differ by CH_2-units.

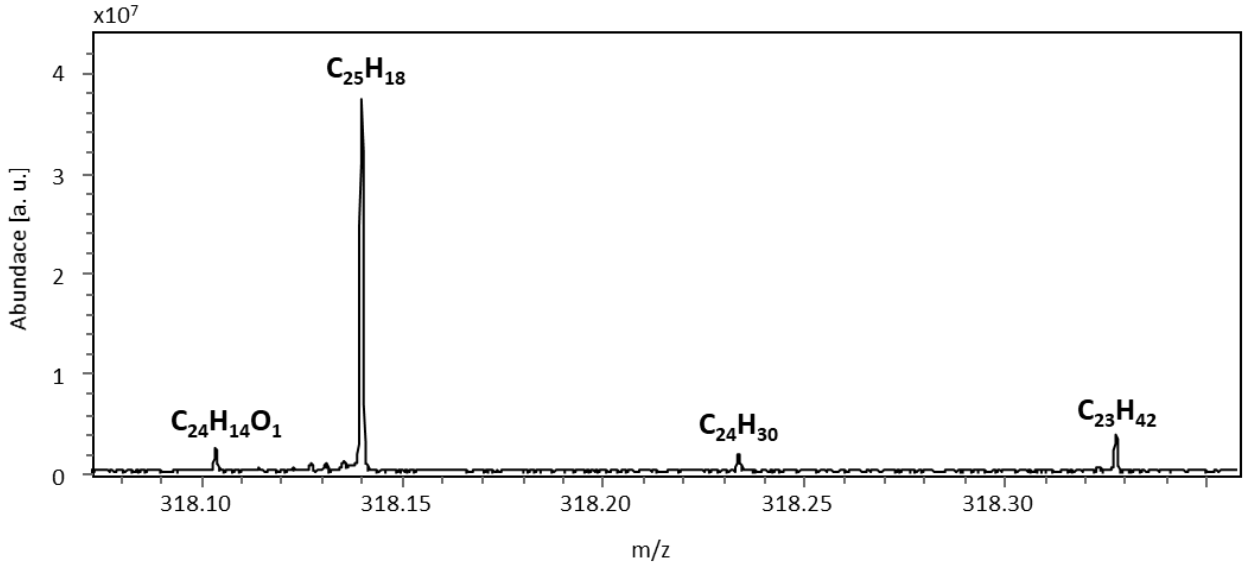

Figure S12. The isobaric complexity is given by enlargement of the nominal mass 318 of sample A.